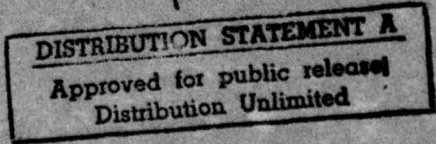
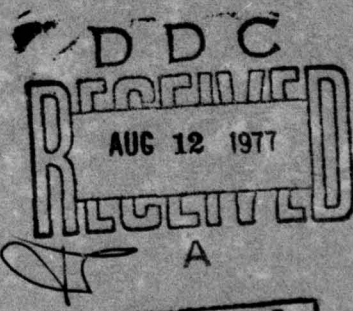
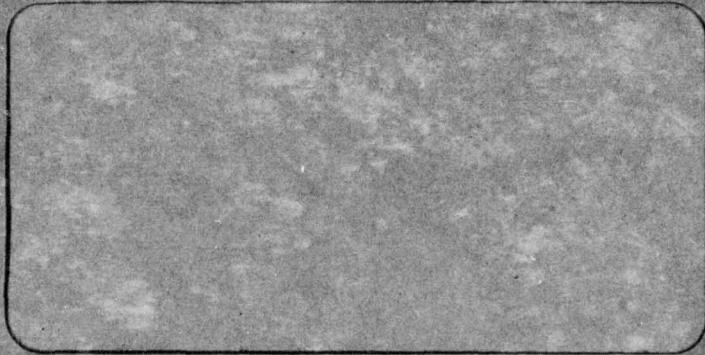
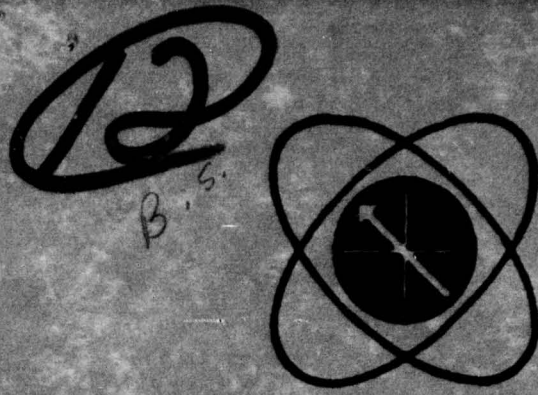


AD No. \_\_\_\_\_  
DDC FILE COPY

ADA042910



MATHEMATICAL SCIENCES NORTHWEST, INC.  
P.O. BOX 1887      BELLEVUE, WASHINGTON 98009

5 May 1977

Program Code Number TE20  
MSNW-1062

①  
② 14

⑨ SEMI-ANNUAL REPORT

⑩ TITLE: KINETIC STUDIES FOR XeF and KrF LASERS

⑪ Contract Number: N00014-76-C-1066

May 1977

⑫ May 77

DARPA Order-1806

Effective Date: 1 September 1976

Expiration Date: 30 November 1977

Amount: \$99,909

DISTRIBUTION STATEMENT A

Approved for public release;  
Distribution Unlimited

⑬ 21P.

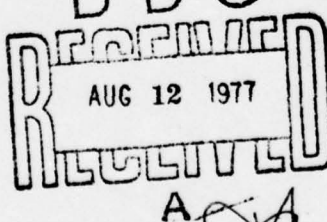
Sponsored By

Defense Advanced Research Projects Agency  
DARPA Order No. 1806

Principal Investigator:

⑭ 10 R. E. Center (206) 827-0460  
C. H. Fisher (206) 827-0460

Scientific Officer:



Director, Physics Programs  
Physical Sciences Division  
Office of Naval Research  
Department of the Navy  
800 North Quincy Street  
Arlington, Virginia 22117

MATHEMATICAL SCIENCES NORTHWEST, INC.  
P. O. Box 1887  
Bellevue, Washington 98009

The views and conclusions contained in this document are those of the authors and should not be interpreted as necessarily representing the official policies, either expressed or implied, of the Defense Advanced Research Projects Agency or the U. S. Government.

404058

SK

## TABLE OF CONTENTS

SECTION	PAGE
I      INTRODUCTION	1
II     EXPERIMENT	3
2.1. Photolysis Cell and Gas Handling	3
2.2. Flashlamp	5
2.3. XeF Laser	8
2.4. Detector	10
III    RESULTS	13
IV    SUMMARY	16
REFERENCES	17

ACCESSION NO.	
NTIS	White Section <input checked="" type="checkbox"/>
DDC	BUU Section <input type="checkbox"/>
UNANNOUNCED	
JUSTIFICATION	
<i>Letter on file</i>	
BY	
DISTRIBUTION/AVAILABILITY CODES	
Dist.	AVAIL. END OR SPECIAL
<i>A</i>	

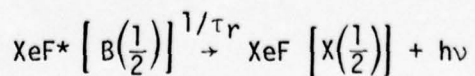
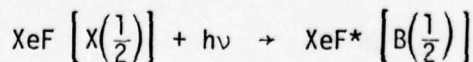
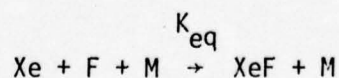
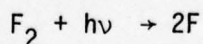
## LIST OF FIGURES

FIGURE	PAGE
1 Schematic diagram of the laser induced fluorescence experiment.	4
2 Oscilloscope traces of flashlamp current and light output at 3500 Å. The capacitor charge voltage was 10 kV, corresponding to an energy of 50 J/lamp. The current was measured with a Pearson probe and the flashlamp radiation was detected with a vacuum photodiode.	6
3 Schematic diagram of the optical setup for the laser induced fluorescence experiment.	9
4 Oscilloscope traces comparing the vacuum photodiode (ITT F400D S5) and photomultiplier (RCA 1P28) to the XeF laser emission. The 1P28 photomultiplier was equipped with a low inductance base as described in the text. The 1P28, although slightly slower than the photodiode, quite accurately reproduces the XeF laser pulse.	12
5 XeF fluorescence at 3533 Å for He + 4% Xe + 0.13% F <sub>2</sub> gas mixture at total pressure of (a) 760 torr and (b) 500 torr. The photodiode response to the XeF laser emissions precedes the photomultiplier response to the fluorescence due to the transit time of the electrons in the photomultiplier.	14

## SECTION I INTRODUCTION

In the last few years there has been intense interest in the rare gas halide lasers because they have been shown to have the potential for high-efficiency, scalability to large volumes and high power levels, and transmission through the atmosphere. The optimization of lasing performance and the scaling to large systems requires a kinetic model of the rare gas halogen system which incorporates the relevant mechanisms for the excitation and destruction of the upper and lower laser levels. There has been considerable experimental and theoretical investigation of the possible kinetic mechanisms leading to the formation of the electronically excited upper state. However, very little information on the radiative lifetime of the upper state or the rate constants for destruction processes has emerged. As a result, it is difficult to estimate the saturation flux or to optimize gas mixtures as a function of total pressure.

The goal of this program is to measure both the radiative lifetime and the collisional quenching rate coefficients for the XeF and KrF upper laser levels. Our approach is to excite a fraction of the ground state molecules in a cell using a short-pulse XeF or KrF laser. The ground state molecules are prepared by flash dissociating a mixture of  $F_2$  and either Xe or Kr plus a monatomic diluent and then allowing the molecular XeF to come to equilibrium with the free atom densities. The sequence of reactions for XeF is as follows:



This approach has the advantage over discharge and electron beam techniques that there will be no residual excited atomic states formed that can interfere with the subsequent fluorescence decay measurement. In addition, by selecting the wavelength of the XeF laser, it is possible to excite only specific vibrational levels of the  $B(1/2)$  upper laser level and to follow the subsequent decay of this specific state without interference.

## SECTION II EXPERIMENT

### 2.1 Photolysis Cell and Gas Handling

A schematic diagram showing the experimental arrangement is presented in Figure 1. The photolysis cell is constructed from quartz tubing with four UV-grade quartz windows arranged in a cross configuration. The cell is mounted inside a double ellipsoidal aluminum reflector with the long arm of the cross located on the common axis of the two ellipses. Two linear flashlamps are located on the other axes of the ellipses, one above and one below the plane of the cross. The exciting laser beam traverses the cell parallel to the flashlamps, while the fluorescence is viewed perpendicular to the exciting beam through a window on the cell. The cell is evacuated by an oil diffusion pump equipped with an anti-creep, liquid nitrogen cooled baffle. Gas samples are introduced to the cell through a high purity stainless steel manifold which was passivated with  $F_2$  before use.

Gas mixtures for the experiment are made up on a separate diffusion pumped manifold and then transferred to the photolysis cell apparatus in stainless steel bottles equipped with demountable high vacuum fittings. This high purity manifold, which was previously used for preparing XeF and KrF laser gas mixtures, has been enlarged so that up to six gas mixtures can be prepared simultaneously. It has also been equipped with demountable high vacuum fittings utilizing metal gaskets so that the bottles containing the mixtures to be photolyzed can be removed and transferred to the high vacuum manifold connected to the photolysis cell. The inertness of the manifold was checked by making up Ar +  $F_2$  mixtures and then verifying the nominal  $F_2$  concentration using vacuum ultraviolet absorption.

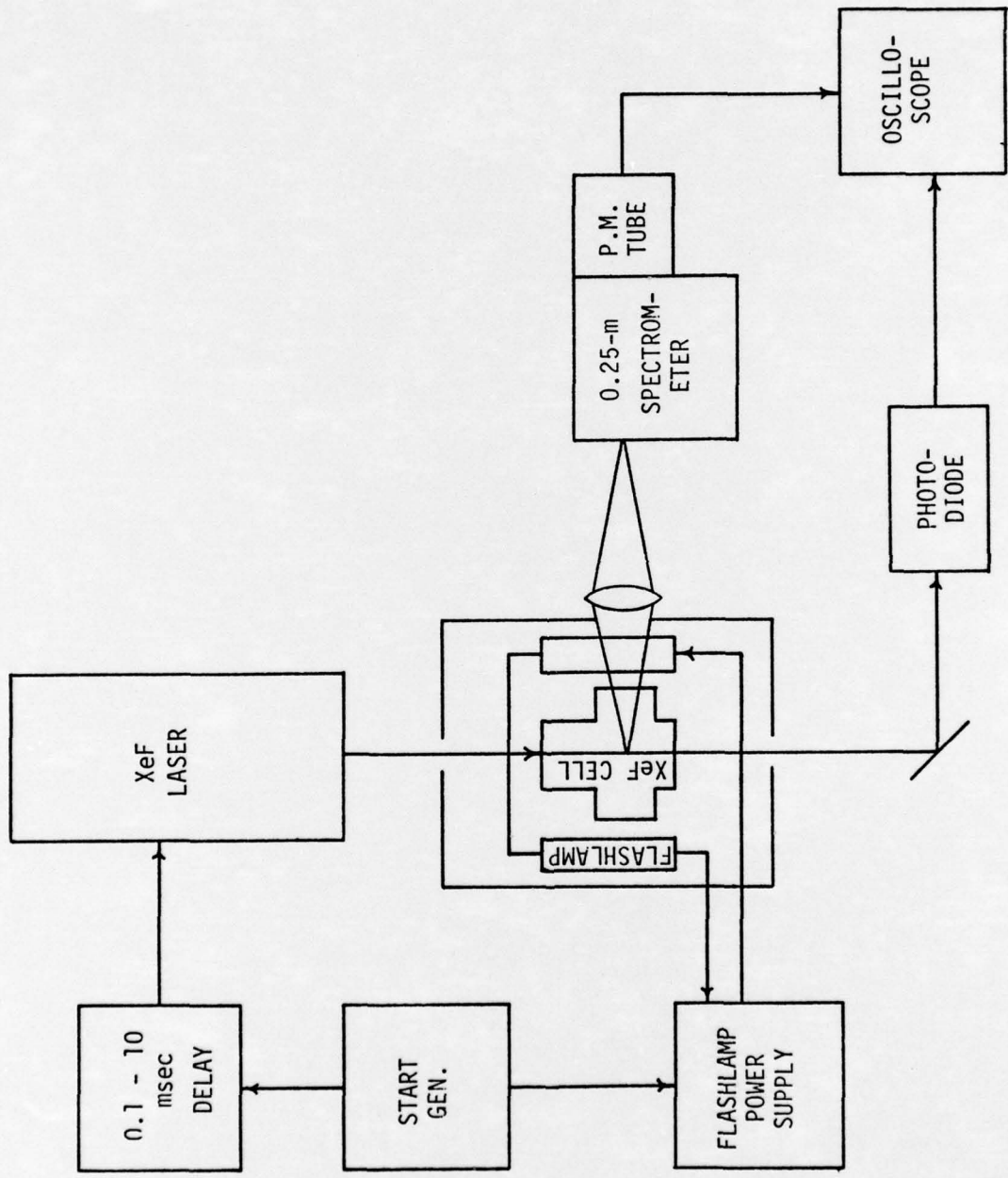


Figure 1. Schematic diagram of the laser induced fluorescence experiment.

## 2.2 Flashlamps

The flashlamps originally chosen for these experiments (Xenon N-734C) have a spectral distribution which peaks in the region of the  $F_2$  continuous absorption band at 2800 Å. The flashlamps are connected in series electrically and triggered by applying a voltage higher than the anode to cathode breakdown potential. The power supply consists of a 2- $\mu$ F capacitor controlled by a triggered spark gap which delivers approximately 50 J to each lamp for a charge voltage of 10 kV. Care has been taken in the design of the flashlamp circuit to minimize the inductance in order to maximize the UV light output. The capacitor, spark gap, and cable assembly contribute approximately 125 nH to the circuit inductance, while the loop containing the two flashlamps in series contributes about 300 nH. This results in a circuit time constant  $\tau = \sqrt{LC} \sim 1 \mu$ sec, which should be about one-third of the electrical pulse width. Oscilloscope traces showing the time history of the current through the flashlamps and the light output at 3500 Å are presented in Figure 2.

Using the calibration of the vacuum photodiode (ITT F4000 S-5) and taking into account the appropriate geometric factors, it is possible to estimate the time-integrated photon flux emitted by the flashlamps. This procedure yields a value of 20 mJ/cm radiated in a 100 Å interval centered at 3500 Å for a peak current of 5 kA through the flashlamps. This corresponds to a time-integrated photon flux of  $3.5 \times 10^{16}$  photons/cm/100 Å. For optically thin conditions, which will apply in this experiment, the dissociation fraction  $[F]/2[F_2]$  is independent of the  $F_2$  concentration and is given by

$$\frac{1}{2} \frac{[F]}{[F_2]} = \int \sigma(v) \phi(v) dv$$

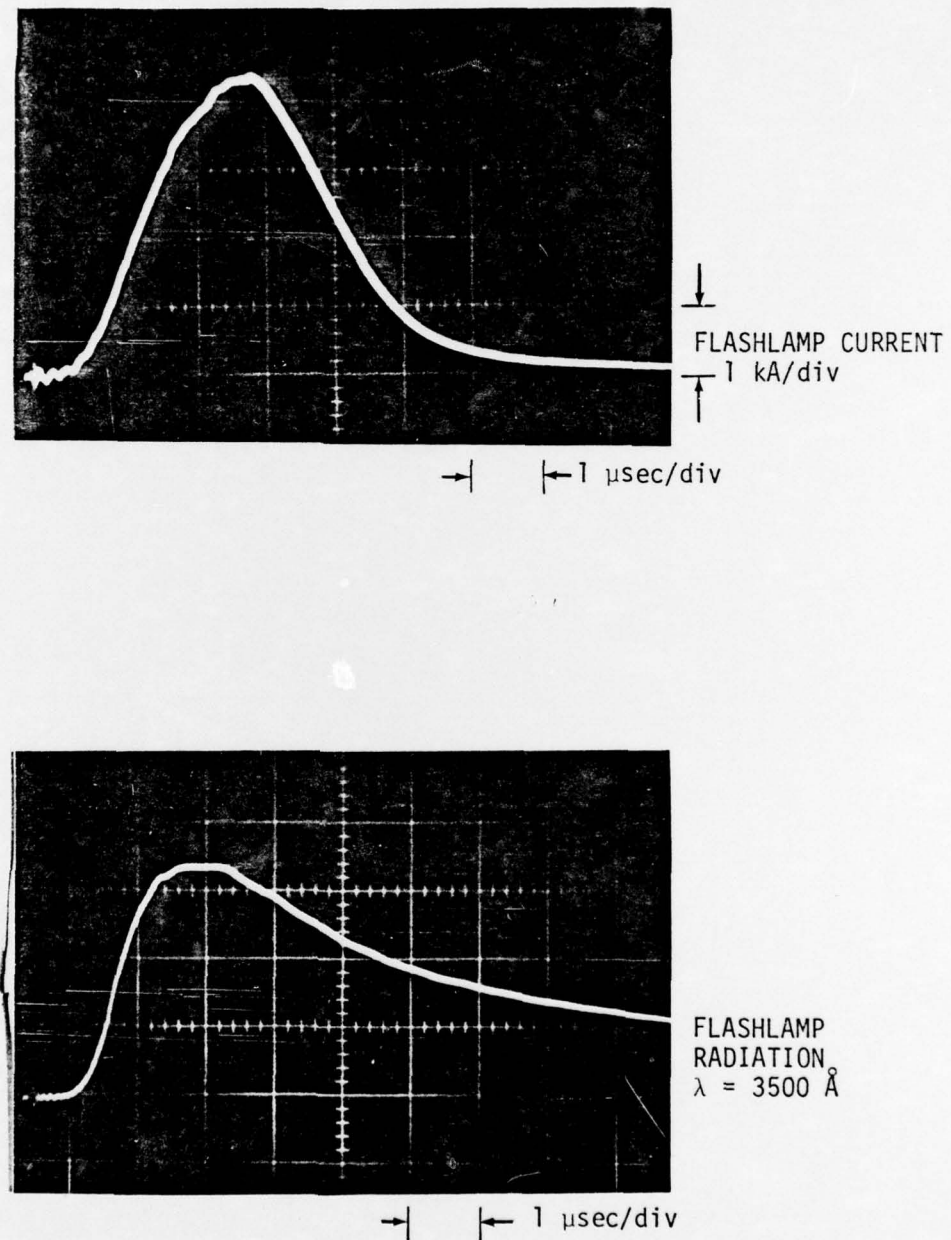


Figure 2. Oscilloscope traces of flashlamp current and light output at 3500 Å. The capacitor charge voltage was 10 kV, corresponding to an energy of 50 J/lamp. The current was measured with a Pearson probe and the flashlamp radiation was detected with a vacuum photodiode.

where  $\sigma(v)$  is the  $F_2$  absorption cross section and  $\phi(v)$  is the time-integrated photon flux from the flashlamp. If it is assumed that the light is uniformly reimaged throughout the 2-cm diameter cell, then the flux density in the cell will be approximately  $1 \times 10^{16}$  photons/cm<sup>2</sup>/100 Å (the light flux density has been doubled because there are two flashlamps). Assuming that this flux density is constant from 2500 Å to 3500 Å and using an average absorption cross section for  $F_2$  of  $10^{-20}$  cm<sup>2</sup>, the fraction of  $F_2$  dissociated is estimated to be about  $10^{-3}$ .

However, at this energy loading (50 J/lamp), the flashlamps failed after approximately 100 shots. We then changed our capacitor to 0.1  $\mu$ F and reduced the energy loading to 25 J/lamp; under these conditions, the new lamps survived for several hundred shots without failure. We have subsequently switched to another manufacturer's lamp (ILC 4D3) with the same arc length and have obtained reliable operation at energy loadings up to 100 J/lamp. The current through these lamps is slightly underdamped with a full width at half maximum of 2.5  $\mu$ sec and a peak value of 11 kA. This has resulted in higher UV output and a larger  $F_2$  dissociation fraction.

Since there is evidence that suggests that the UV light output occurs mainly during the first few hundred nanoseconds of the flash,<sup>1</sup> we shortened our current pulse in an effort to increase the UV output. This was accomplished by changing the 2- $\mu$ F capacitor to 0.1  $\mu$ F and using higher charge voltages to keep the energy loading high. This shortened the current pulse to approximately 600 nsec, but the waveform became severely underdamped. The UV output at 2300 Å and 2800 Å was monitored relative to that at 3500 Å for both capacitors. While the absolute UV output did not increase when the 0.1- $\mu$ F capacitor was used, the UV output relative to that at 3500 Å did increase, resulting in an increase in the efficiency of UV production. However, since the absolute UV output must be maximized for these experiments, we have used the 2- $\mu$ F capacitor with an energy loading of 100 J/lamp.

### 2.3 XeF Laser

The XeF laser used in this work is a Blumlein-driven discharge laser equipped with a flashboard preionization circuit. The UV light from the flashboard creates enough ionization in the gas to prevent arc formation at the higher pressures needed to obtain a short laser pulse. Photodiode measurements indicate that the UV output from the flashboard reaches a maximum at approximately 200 to 300 nsec after initiation. Optimum performance of the XeF laser is obtained by firing the main discharge at the peak of the UV preionization pulse.

In our preliminary experiments, the scattered light levels at 3511 Å, and 3533 Å were found to be extremely high. This problem was alleviated by inserting a grating in the XeF laser cavity. The grating was tuned so that the laser operated at 3511 Å [ $\text{XeF } (B(1/2)v'=0 \rightarrow X(1/2)v''=2)$ ] while the spectrometer was tuned to 3533 Å [ $\text{XeF}(B(1/2)v'=0 \rightarrow X(1/2)v''=3)$ ]. It was still necessary to take careful precautions to keep 3511 Å scattered laser light from entering the spectrometer with the relatively wide slits used in these experiments. A schematic diagram of the optical layout that gave the best results is shown in Figure 3. The highly divergent and poorly defined XeF laser beam is brought to a focus by the first lens ( $f = 30$  cm). A slit is placed at the focus to remove all but the most intense portion of the beam. The slit was sized just larger than the burn pattern made on blackened polaroid film. The second lens ( $f = 10$  cm) then refocuses the laser inside the photolysis cell. Several other apertures, both on the laser beam and the viewing optics, were found to be useful in minimizing the scattered light.

With the cavity formed by the grating and a 60 percent transmission curved mirror and with a He + 1% Xe + 0.3%  $\text{NF}_3$  gas mix at 1 atm, the XeF laser pulse had a full width at half maximum of 15 to 20 nsec with a long fall time. Efforts to shorten the decay of the laser pulse by operating this gas mixture at higher pressure were not successful because arcing occurred in the discharge. However, it was found possible to shorten the laser pulse by replacing the 60 percent transmission curved mirror with an uncoated fused

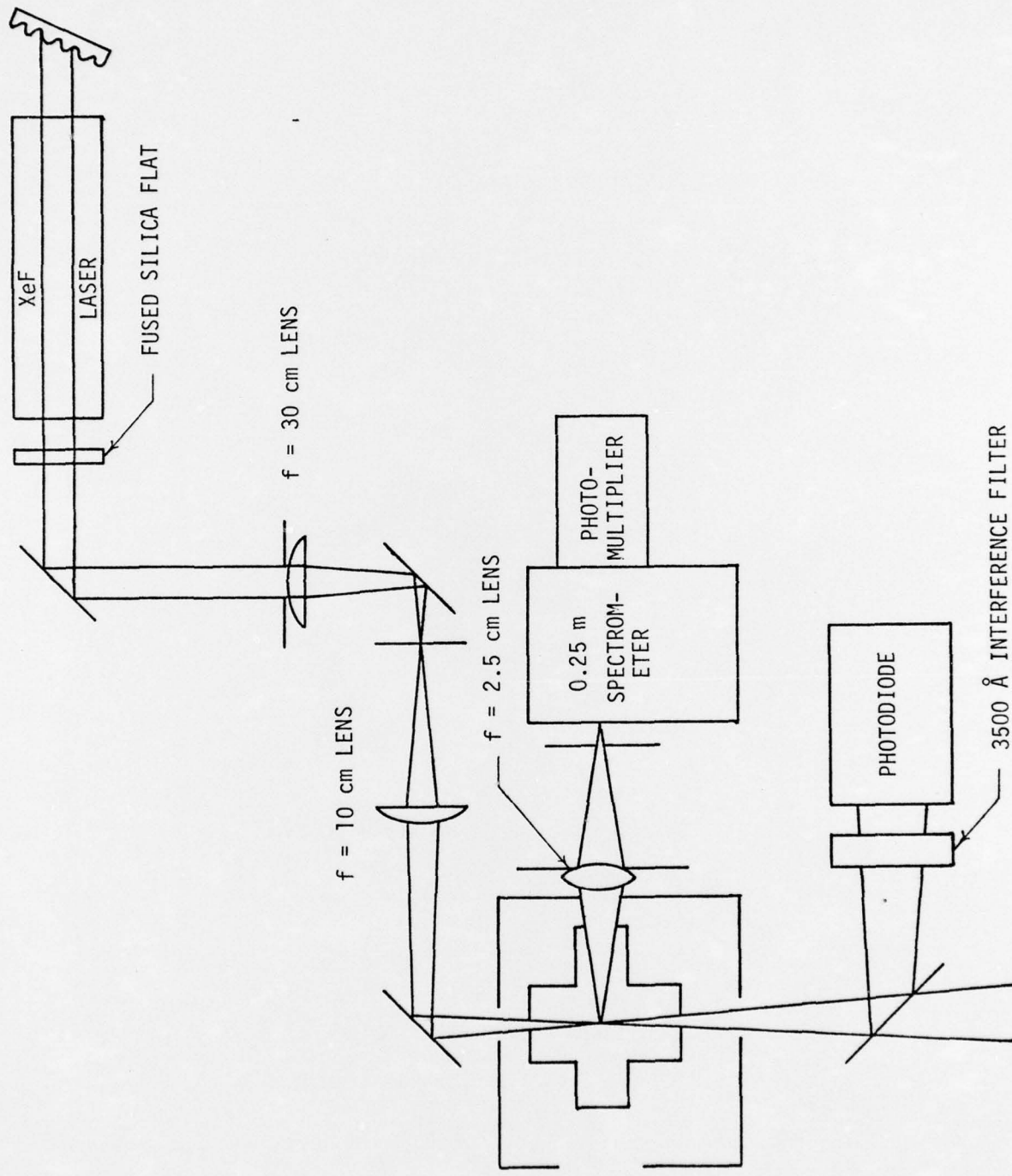


Figure 3. Schematic diagram of the optical setup for the laser induced fluorescence experiment.

silica flat. The pulse could be shortened a little more by slightly mis-aligning the fused silica flat. The pulse energy with this configuration was 3 to 4 mJ.

Better results were obtained by switching to He + 1% Xe + 0.5% F<sub>2</sub> gas mixtures at pressures of 1.7 to 2 atm. The laser pulse duration is longer than with NF<sub>3</sub> mixtures, but the fall time is shorter. The output energy was about 10 to 15 mJ with a pulse duration of 10 nsec (FWHM) and a fall time (0 - 100%) about the same. Mixtures containing higher F<sub>2</sub> concentrations (up to 2 percent) were also tried; however, they decreased the pulse energy without substantially shortening the laser decay time.

#### 2.4 Detector

The detection scheme for the XeF fluorescence consists of a 0.25 m Jarrel-Ash spectrometer to provide wavelength selection, followed by a 1P28 photomultiplier. The temporal profile of the exciting laser is monitored by placing a fused silica flat in the beam after it leaves the fluorescence cell and reflecting a few percent of the laser light onto a vacuum photodiode (ITT F4000 S5). The photomultiplier and photodiode responses are then displayed on a Tektronix 7844 oscilloscope ( $t_r \sim 1$  nsec) and photographed on Polaroid film. Severe electrical noise generated by the Blumlein laser discharge and rail switch were picked up by the photomultiplier and photodiode even though they each had shielded housings. This problem was alleviated by enclosing the entire Blumlein laser in a frame covered by two layers of brass screen. It was also necessary to place a second shielded enclosure around the photomultiplier and the photodiode, to place their power supplies in the screen box with the oscilloscope, and to use doubly-shielded connecting cables between the screen box and the detectors. After all these measures were implemented, electrical noise was no longer a problem even on the most sensitive oscilloscope scale (5 mV).

The time response of the photomultiplier and tube base assembly was checked by setting the spectrometer to view the scattered laser light at 3511 Å and comparing the photomultiplier output with that of the vacuum photodiode. The ITT F4000 S5 vacuum photodiode has a rise time of 0.5 nsec and a fall time of 0.8 nsec which is fast enough to faithfully reproduce the laser temporal profile. The first photomultiplier tried was an RCA C31034 with a commercially wired tube base and housing (Products for Research Model PR-2200-RF). According to the manufacturer, this photomultiplier has a risetime of 2.5 nsec or less. The tube did reproduce the rise of the laser pulse accurately; however, the fall was considerably longer than the photodiode and showed evidence of ringing. An RCA 1P28 photomultiplier ( $t_r \leq 2$  nsec) with a tube base and housing constructed in our laboratory was evaluated next. This tube had a faster fall time than the C31034 but still considerably slower than the photodiode. It also exhibited abrupt declines in output current at high signal levels in spite of the fact that the last few dynodes had large bypass capacitors.

These difficulties were eliminated by removing the phenolic base from the 1P28 and soldering the pins directly to a low inductance tube base constructed on printed circuit board as described by Lytle.<sup>2</sup> According to Lytle, a 1P28 with a tube base wired in this manner exhibits a rise time of 1.4 nsec and a fall time of 3.7 nsec. Figure 4 presents oscilloscope traces comparing the photodiode and 1P28 responses to scattered laser light. The photomultiplier is slightly slower than the photodiode on the fall of the pulse, but the overall reproduction is quite accurate. The 1P28 output remained linear up to currents of approximately 100 mA. At higher output currents, saturation effects were apparent; however, there was no evidence of the abrupt declines in signal observed previously, even when the tube was heavily saturated.

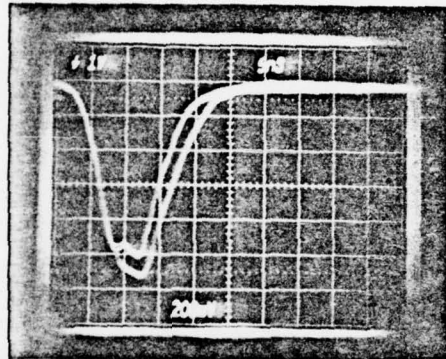


Figure 4. Oscilloscope traces comparing the vacuum photodiode (ITT F400D S5) and photomultiplier (RCA 1P28) to the XeF laser emission. The 1P28 photomultiplier was equipped with a low inductance base as described in the text. The 1P28, although slightly slower than the photodiode, quite accurately reproduces the XeF laser pulse.

### SECTION III

#### RESULTS

Oscilloscope traces showing fluorescence emission at  $3533 \text{ \AA}$  from gas mixtures containing He + 6.6% Xe + 0.13%  $\text{F}_2$  at total pressures of 760 and 500 torr are shown in Figure 5. The total input energy to the flashlamps was 200 J, and the time delay between the photolysis flash and the exciting laser was 0.5 msec. We have been able to obtain fluorescence signals at delays ranging from 0.1 to 5 msec, although the maximum fluorescence signals were obtained with delays of 0.2 to 0.5 msec. No fluorescence signal was obtained unless both the flashlamps and the XeF laser were fired in combination. Two blank mixtures were also utilized to verify that the fluorescence was from  $\text{XeF}^*$ ; Xe was omitted from one mixture, while  $\text{F}_2$  was omitted from the other. Neither of these mixtures produced any fluorescence emission.

An attempt was made to increase the fluorescence emission signal by flash dissociating  $\text{XeF}_2$  to form XeF molecules directly.  $\text{XeF}_2$  has a weak absorption band peaked at approximately  $2300 \text{ \AA}$  with a maximum cross section of about  $2 \times 10^{-19} \text{ cm}^2$ .<sup>3</sup> If this absorption band is continuous, then every dissociation yields an XeF molecule directly rather than converting a small equilibrium fraction of the F atoms formed from  $\text{F}_2$  dissociation into XeF. We tried  $\text{XeF}_2$ , both by itself at pressures of 1 to 3 torr and also at 3 torr with 100 torr of He diluent. Fluorescence was obtained, but it was considerably weaker than that obtained with He + Xe +  $\text{F}_2$  mixtures. The fluorescence signal obtained was so weak that the time history suffered severe distortion due to statistical fluctuations because too few photoelectrons were produced within the photomultiplier resolving time ( $\sim 3 \text{ nsec}$ ). The weak fluorescence is probably due to the poor overlap of the flashlamp spectral distribution with the short wavelength absorption of  $\text{XeF}_2$ .

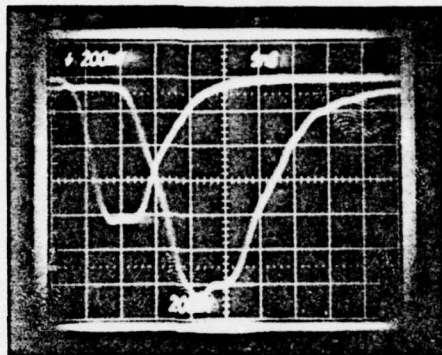
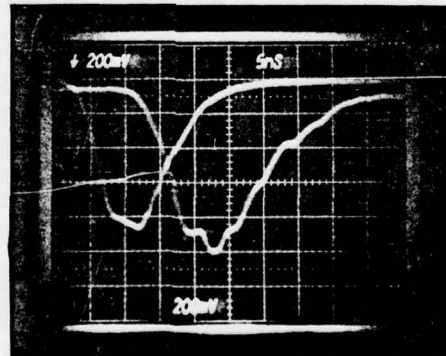
(a)  $p = 760$  torr He + 4% Xe + 0.13%  $F_2$ (b)  $p = 500$  torr He + 4% Xe + 0.13%  $F_2$ 

Figure 5. XeF fluorescence at  $3533 \text{ \AA}$  for a He + 4% Xe + 0.13%  $F_2$  gas mixture at total pressures of (a) 760 torr and (b) 500 torr. The photodiode response to the XeF laser emissions precedes the photomultiplier response to the fluorescence due to the transit time of the electrons in the photomultiplier.

It is apparent from Figure 5 that the exciting laser pulse is not short compared to the fluorescence decay. Primarily for this reason a semi-log plot of the fluorescence decay does not fit a straight line, indicating an exponential decay, but shows evidence of a changing slope. In order to obtain the decay constant for the fluorescence, it is necessary to take into account the exciting laser pulse. The differential equation describing the production and loss of  $\text{XeF}^*$  is

$$\frac{d}{dt} [\text{XeF}^*] = P(t) - [\text{XeF}^*] \left( \frac{1}{\tau_r} + \sum_i k_{qi} Q_i \right) = P(t) - \Gamma [\text{XeF}^*]$$

where  $P(t)$  is the exciting laser pulse and  $\Gamma = \frac{1}{\tau_r} + \sum_i k_{qi} Q_i$  is the effective decay constant for the  $\text{XeF}^*$ . This equation has the solution

$$[\text{XeF}^*(t)] = e^{-\Gamma t} \int_0^t P(T) e^{\Gamma T} dT$$

The most straightforward way to obtain  $\Gamma$  from the fluorescence decay is to obtain an initial estimate of  $\Gamma$  from a semi-log plot of the fluorescence emission as a function of time. This value of  $\Gamma$  is used to numerically evaluate the above integral and the resulting calculated decay compared with the measured decay. This process is repeated until a  $\Gamma$  is obtained which gives a good fit to the experimental data. We are presently writing a simple computer program to evaluate this integral.

#### SECTION IV SUMMARY

By flash photolyzing mixtures of Xe and  $F_2$  diluted in Ar and He, we have obtained state selective, laser-induced fluorescence from the  $B(1/2)v' = 0 \rightarrow X(1/2)v'' = 3$  transition of XeF. The mixtures utilized thus far yield decay time constants, which contain contributions both from quenching and radiative decay, of less than 10 nsec. These decays are not long compared to the exciting laser pulse so that the observed decay is the convolution of the exciting laser pulse with the radiative and collisional decay. We are writing a simple computer program to do this convolution so that an accurate value of the decay constant can be extracted from the observed fluorescence decay. By measuring the decay constant as a function of concentration of each species in the mixtures, both the rate coefficient for quenching by that species and the radiative lifetime of the  $XeF[B(1/2)v' = 0]$  state can be obtained.

#### REFERENCES

1. J.B. Trenholme and J.L. Emmett, Ultraviolet Output from Pulsed Short Arcs, NRL Memorandum Report 2427, April 1972.
2. J.M. Harris, F.E. Lytle, and T.C. McCain, Anal. Chem. **48**, 2095 (1976).
3. J. Jortner, E.G. Wilson, and S.A. Rice, "Theoretical and Experimental Studies of the Electronic Structure of the Xenon Fluorides," in Hyman: Noble-Gas Compounds, Chicago: University of Chicago Press, p. 359 (1963).